豊，阿部祐士，岩井克成，山田孝子，鷲見幸彦，加知輝彦，川島隆太，福田　寛　パーキンソン病における視覚情報処理脳機能の変化，レイヴン色彩マトリックス検査とH2O脳血流賦活PET検査による検討．心の健康科学福山班班会議　2004年1月6日　大府市

22) 河津 省司，　右代谷 昇，　加藤 隆司，　二橋 尚志，　伊藤 健吾．　FDG-PETおよびIMPを用いた多変量解析による正常者とアルツハイマー病患者鑑別の試み，　第 44 回　日本核医学会総会 京都国際会議場　京都市 2004 年 11 月 4-6 日

23) 加藤隆司，伊藤健吾，河津省司，齋藤敦子，籏野健太郎，吉村公美子，鷲見幸彦，阿部祐士，新畑　豊，岩井克成，二橋尚志「脳糖代謝の正常変動に関する検討」，第44回　日本核医学会総会 京都国際会議場　京都市 2004 年 11 月 4-6 日

24) 吉村公美子，加藤隆司，河津省司，阿部祐士，新畑　豊，岩井克成，田中郁子，加藤力雄，二橋尚志，伊藤健吾　IMP 脳血流 SPECT 検査によるアルツハイマー病の自動 ROI 数値診断の試み　日本放射線技術学会 第 32 回秋期学術大会　2004 年 10 月 21-23 日　大阪

25) 吉村公美子，加藤隆司，河津省司，田中郁子，伊藤健吾，加藤力雄，二橋尚志，阿部祐士，新畑豊，岩井克成．　自動 ROI によるアルツハイマー病の IMP 脳血流 SPECT 数値診断の試み　第 44 回日本核医学会総会　2004 年 11 月 4-6 日　京都

26) 二橋尚志，加藤隆司，河津省司，吉村公美子，伊藤健吾，阿部祐士，新畑豊，岩井克成，武田章敬，鷲見幸彦．　3D-SSP を用いたアルツハイマー型痴呆の診断能に関する FDG-PET と IMP-SPECT の比較．第 44 回日本核医学会総会　2004 年 11 月 4-6 日　京都

27) パーキンソン病におけるドーパミン神経系の障害と脳糖代謝の関連に関する検討ー2
新畑 豊、阿部祐士、岩井克成、山田孝子、鷲見幸彦、加知輝彦、加藤隆司、伊藤健吾
第45回日本神経学会総会，2004年5月14日　東京．

28) 阿部祐士，鷲見幸彦，岩井克成，新畑　豊，山田孝子，加知輝彦，加藤隆司，伊藤健吾，祖父江元
パーキンソン病における Mini Mental State Examination の検討　日本神経学会総会，2003 年 5 月 17 日，横浜

29) 岩井克成，阿部祐士，鷲見幸彦，新畑　豊，山田孝子，加知輝彦，加藤隆司，伊藤健吾，祖父江元
パーキンソン病における 18F-DOPA および 18F-FDG PET 画像の縦断的研究
日本神経学会総会，2003 年 5 月 16 日，横浜

30) 加藤隆司，伊藤健吾，河津省司，齋藤敦子，籏野健太郎，志田原美保，桃崎壮太郎，川角保広，阿部祐士，鷲見幸彦，新畑　豊，岩井克成，山田孝子，加知輝彦．
健常者の脳糖代謝の加齢性変化に関する検討
第43回日本核医学会総会 2003年10月27日　東京

31) Nagano-Saito A, Arahata Y, Abe Y, Washimi Y, Yamada T, Nakamura A, Iwai K, Ito K, Kachi T, Hatano K, Kato T, Kawasumi Y, Kato R, Aihara Y, Ogawa M, Tsuji A, and Kawatsu S:
Mesolimbic dopaminergic system in Parkinson's disease without dementia. - A PET study-
Molecular Imaging and Drug Development. Jan.30-Feb.1, 2002, Hamamatsu, Japan.

32) 梶田泰一、金桶吉起、川上治、前澤　聡、臼井直敬、吉田純　微小電位記録とコンピューター支援技術を併用したパーキンソン病に対する定位的淡蒼球破壊術　第４０回日本・機能神経外科学会　平成１３年１０月２２、２３日、岡山

33) 梶田泰一、金桶吉起、前澤　聡、遠藤乙音、川上　治、吉田　純　視床下核を電気生理学的に同定するための schaltenbland and wahren 3D アトラスの作成　第 41 回日本定位・機能神経外科学会　平成１４年９月３０日、１０月１日、松本

34) 梶田泰一、金桶吉起、前澤　聡、遠藤乙音、吉田　純　パーキンソン病視床下核深部刺激術に有用な schaltenbland and wahren 3D アトラスの作成　第 61 回日本脳神経学会総会　平成１４年１０月２－４日、松本

35) 前澤聡、金桶吉起、梶田泰一、中山敦雄、三澤伸明、遠藤乙音、吉田純　6-OHDA パーキンソン病ラットを用いた慢性視床下核電気刺激モデルの作成　第 18 回不随意運動研究会　名古屋　７月２５日

36) 前澤聡、金桶吉起、梶田泰一、中山敦雄、三澤伸明、遠藤乙音、吉田純　6-OHDA パーキンソン病ラットを用いた慢性視床下核電気刺激モデルの作成　第 15 回関東機能的脳外科カンファレンス　東京　９月７日

37) 前澤聡、金桶吉起、梶田泰一、遠藤乙音、吉田純線状体の Tonically Active Neurons(TANs)の性格—Parkinson 病、ジストニア患者においての検討　第 41 回日本定位機能神経外科学会　松本　9月 30 日、10 月 1 日

38) 前澤聡、金桶吉起、梶田泰一、中山敦雄、三澤伸明、遠藤乙音、吉田純　6-OHDA パーキンソン病ラットを用いた慢性視床下核電気刺激モデルの作成　第 61 回日本脳神経外科総会　松本　１０月２－４日

39) 前澤聡、金桶吉起、梶田泰一、臼井直敬、中山敦雄、三澤伸明、遠藤乙音、吉田純　視床下核刺激治療(STN-DBS)の神経細胞保護効果—ラッ

ト 6-OHDA モデルでの検討　第 5 回東海定位脳治療研究会　名古屋　１２月６日
40) Chronic Stimulation to the Subthalamic Nucleus in Rat Hemiparkinsonian Model:Behavioral and Immunohistopathological Evaluation Revealed Neuroprotective
Effects against Degeneration of Dopaminergic Neurons
41) Satoshi Maesawa, Yoshiki Kaneoke, Yasukazu Kajita, Naotaka Usui,
Nobuaki Misawa, Atsuo Nakayama, Jun Yoshida
53th Annual Meeting of Congress of Neurological surgeons, Denver, Colorado,
October 18 - 23, 2003 Denver, USA
42) Kajita Y, Maesawa S, Endoh O, Wakabayashi T, Yoshida J
The usefulness of subcortical monitoring using MEP following cortical or transcranial electrical stimulation in the operation of the cerebral lesions near pyramidal tract or the central sulcus
57th American epilepsy society annual meeting Dec. 5-10 2003 Boston, USA
43) 梶田泰一、金桶吉起、前澤　聡、臼井直敬、遠藤乙音、吉田　純　視床下核を電気生理学的に同定するための schaltenbland and wahren 3D アトラスの作成　第２６回日本脳神経 CI 学会
平成１５年２月７，８日、名古屋
44) 遠藤乙音、梶田泰一、前澤聡、吉田純
Parkinson 病、てんかん患者に於ける三次元脳血流の検討　第26回　日本脳神経 CI 学会　平成１５年２月７，８日、名古屋
45) 梶田泰一、金桶吉起、前澤　聡、臼井直敬、遠藤乙音、吉田　純　定位的淡蒼球破壊術後２３日目に、軽度の片麻痺症状が出現した症例
第１６回　関東機能的脳外科カンファレンス
平成１５年４月５日、東京
46) 梶田泰一、金桶吉起、前澤　聡、臼井直敬、遠藤乙音、吉田　純　定位的淡蒼球深部刺激術における電極至適留置部位の検討　第１９回不随意運動研究会　平成１５年７月２４日、名古屋
47) 梶田泰一、金桶吉起、前澤　聡、臼井直敬、遠藤乙音、竹林成典、吉田　純　脳深部刺激術の DBS リード留置手技における工夫　第１７回関東機能的脳外科カンファレンス
平成１５年９月６日、東京
48) 梶田泰一、金桶吉起、前澤　聡、竹林成典、遠藤乙音、臼井直敬、吉田　純　パーキンソン病における淡蒼球深部刺激術の至適電極留置部位の検討　第４２回日本定位・機能神経外科学会
平成１５年９月２９、３０日、仙台
49) 前澤聡、金桶吉起、梶田　泰一、三澤　伸明、臼井　直敬、中山　敦雄、吉田　純視床下核慢性刺激の黒質ドーパミン細胞に対する保護効果−ラットパーキンソンモデルでの検討　第 42 回日本定位、機能神経外科学会　平成１５年９月２９，３０日、仙台
50) 前澤聡、金桶吉起、梶田　泰一、三澤　伸明、臼井　直敬、中山　敦雄、吉田　純視床下核慢性刺激の黒質ドーパミン細胞に対する保護効果−ラットパーキンソンモデルでの検討　第 62 回日本脳神経外科学会総会　平成15年10月1—3日、仙台
51) 梶田泰一、齋藤　清、原　政人、前澤　聡、青島千洋、竹林成典、遠藤乙音、臼井直敬、水野正明、若林俊彦、吉田純　手術支援情報ネットワークシステムにささえられた脳・脊髄外科手術：術中電気生理学的情報の有用性　第８回日本脳腫瘍の外科学会　平成１５年１１月７、８日、那覇
52) Kajita Y, Kaneoke Y, Tekebayashi S, Noda H, Bundo M, Washimi Y, Kato R, Ito K, Yoshida J. Influence of pallidal stimulation on cognitive function in the cases with Parkinson's Disease
The 5th Congress of Asian Society Stereotactic Functional and Computer Assisted Neurosurgery. Nov. 27-30 2004 Kaohsiung, Taiwan
53) Tekebayashi S, Noda H, Kajita Y, Kaneoke Y, Noda H, Yoshida J
The optimal electrode location of the unilateral pallidal stimulation for the Parkinson disease
The 5th Congress of Asian Society for Stereotactic,Functional and ComputerAssisted Neurosurgery. November 27-30,2004, Kaohsiud, Taiwan
54) Noda H, Kajita Y, Kaneoke Y, Tekebayashi S, Yoshida J. Shaitenbland and Wahren 3D atlas for electrophysiological identification of subthalamic nucleus
The 5th Congress of Asian Society for Stereotactic,Functional and ComputerAssisted Neurosurgery
November 27-30,2004,Kaohsiud,Taiwan
55) 梶田泰一、前澤　聡、青島千洋、臼井直敬、竹林成典、遠藤乙音、原　政人、吉田　純
中心溝・錐体路近傍脳腫瘍における経皮質・頭蓋電気刺激運動機能モニタリングの有用性　第６

回人脳機能マッピング学会大会
平成１６年3月２１－２２日、東京
56) 梶田泰一、金桶吉起、前澤　聡、臼井直敬、竹林成典、吉田　純　定位的淡蒼球刺激療法を施行した外傷性ジストニア症例における大脳基底核単一神経活動記録の検討　第２７回日本神経外傷学会　平成１６年3月２６－２７日、東京
57) 梶田泰一、金桶吉起、竹林成典、野田　寛、遠藤乙音、文堂昌彦、鷲見幸彦、加藤隆司、伊藤健吾、吉田　純　パーキンソン病に対する定位的淡蒼球手術前後の高次脳機能評価　第２０回不随意運動研究会　平成１６年７月２２日、名古屋

総　説
1) 阿部祐士, 伊藤健 吾. PET による高次脳機能障害の診断. BIO Clinica 17: 504-507, 2002
2) 新畑　豊, 伊藤健吾, 加藤隆司. パーキンソン病の痴呆. Cognition and Dementia 1;45-49, 2004.
3) 新畑　豊、伊藤健吾、加藤隆司 パーキンソン病の痴呆 Cognition and Dementia vol3 (1);45-49, 2004.

知的所有権の取得状況

なし

II. 研究成果の刊行に関する一覧表

書籍

なし

雑誌

発表者氏名	論文タイトル名	発表誌名	巻号	ページ	出版年
Ito K, Nagano-Saito A, Arahata Y, Nakamura A, Kawasumi Y, Hatano K, Abe Y, YamadaT, Kachi T, Brooks DJ	Striatal and Extrastriatal dysfunction in Parkinson's disease with dementia: a 6-[18F]fluoro-L-dopa PET study	Brain	123	1358-1365	2002
Rakshi JS, Pavese N, Uema T, Ito K, Morrish PK, Bailey DL, Brooks DJ	A comparison of the progression of early Parkinson's disease in patients started on ropinirol or L-dopa an (18)F-dopa PET study	J Neural Transm	109(12)	1433-1443	2002
Kawatsu S, Kato T, Nagano-Saito A, Hatano K, Ito K, Ishigaki T	New Insight into the Analysis of 6-[18F]fluoro-L-DOPA PET Dynamic Data in Brain Tissue without an Irreversible Compartment: Comparative Study of the Patlak and Logan Analysis	Radiation Medicine	21(1)	47-54	2003
Abe Y, Kachi T, Kato T, Arahata Y, Yamada T, Washimi Y, Iwai K, Kawatsu K, Ito K, Yanagisawa N, Sobue G	Occipital hypoperfusion in Parkinson's disease without dementia: correlation to impaired cortical visual processing	J Neurol Neurosurg Psychiatry	74	419-22	2003
Iida Y, Ogawa M, Ueda M, Tominaga A, Kawashima H, Magata Y, Nishimura S, Tsukada H, Mukai T, Saji H	Evaluation of 5-(11)C-methyl-A-85380 as an imaging agent for PET investigations of brain nicotinic acetylcholine receptors	J Nucl Med	45	878-84	2004

雑誌　つづき

発表者氏名	論文タイトル名	発表誌名	巻号	ページ	出版年
Nagano-Saito A, Kato T, Arahata Y, Washimi Y, Nakamura A, Abe Y, Yamada T, Iwai K, Hatano K, Kawasumi Y, Kachi T, Dagher A, Ito K.	Cognitive- and motor-related regions in Parkinson's disease: FDOPA and FDG PET studies.	Neuroimage	22	553-61	2004
Nagano-Saito A, Washimi Y, Arahata Y, Iwai K, Kawatsu S, Ito K, Nakamura A, Abe Y, Yamada T, Kato T, Kachi T.	Visual hallucination in Parkinson's disease with FDG PET	Mov Disord	19	801-806	2004
Maesawa S, Kaneoke Y, Kajita Y, Usui N, Misawa N, Nakayama A, Yoshida J.	Long-term subthalamic nucleus in hemiparkinsonian rats: Neuroprotection of dopaminergic neurons.	J Neurosurg	100	670-687	2004
Nagano-Saito A, Washimi Y, Arahata Y, Kachi T, Lerch JP, Evans AC, Dagher A, Ito K.	Cerebral atrophy and its relation to cognitive impairment in Parkinson disease.	Neurology	64	224-9	2005
Mamede M, Ishizu K, Ueda M, Mukai T, Iida Y, Fukuyama H, Saga Tsuneo, Saji H.	Quantification of Human Nicotinic Acetylcholine Receptors with I-123 5IA SPECT.	J Nucl Med	45	1458-70	2004
Ueda M, Iida Y, Mukai T, Mamede M, Ishizu K, Ogawa M, Magata Y, Konishi J, Saji H.	5-[I-123]Iodo-A-85380: assessment of pharmacological safety, radiation dosimetry and SPECT imaging of brain nicotinic receptors in healthy subjects.	Ann Nucl Med	18	337-44	2004

III. 研究成果の刊行物・別刷

Brain (2002), **125**, 1358–1365

Striatal and extrastriatal dysfunction in Parkinson's disease with dementia: a 6-[^{18}F]fluoro-L-dopa PET study

Kengo Ito,[1] Atsuko Nagano-Saito,[1] Takashi Kato,[1] Yutaka Arahata,[1] Akinori Nakamura,[1] Yasuhiro Kawasumi,[1] Kentaro Hatano,[1] Yuji Abe,[2] Takako Yamada,[2] Teruhiko Kachi[2] and David J. Brooks[3,4]

[1]*Department of Biofunctional Research, National Institute for Longevity Sciences and* [2]*Department of Neurology, Chubu National Hospital, Obu, Japan,* [3]*MRC Clinical Sciences Centre, Imperial College School of Medicine, Hammersmith Hospital, London and* [4]*Institute of Neurology, Queen Square, London, UK*

Correspondence to: Dr Kengo Ito, Department of Biofunctional Research, National Institute for Longevity Sciences, 36-3 Gengo, Morioka-cho, Obu, Aichi Prefecture, 474-8522, Japan
E-mail: kito@nils.go.jp

Summary

We investigated the relative differences in dopaminergic function through the whole brain in patients with Parkinson's disease without dementia (PD) and with dementia (PDD) using 6-[^{18}F]fluoro-L-dopa (^{18}F-dopa) PET and a voxel-by-voxel analysis. The 10 PD and 10 PDD patients were equivalently disabled, having mean scores of 3.2 ± 0.6 and 3.2 ± 0.7, respectively, on the Hoehn and Yahr rating scale. ^{18}F-dopa influx constant (Ki) images of those patients and 15 normal age-matched subjects were transformed into standard stereotactic space. The significant differences between the groups (expressed in mean regional Ki values) were localized with statistical parametric mapping (SPM) on a voxel-by-voxel basis. Compared with the normal group, SPM localized declines of the ^{18}F-dopa Ki bilaterally in the putamen, the right caudate nucleus and the left ventral midbrain for the PD group ($P < 0.01$, corrected). Compared with the normal group, the PDD group showed reduced ^{18}F-dopa Ki bilaterally in the striatum, midbrain and anterior cingulate area ($P < 0.01$, corrected). A relative difference in ^{18}F-dopa uptake between PD and PDD was the bilateral decline in the anterior cingulate area and ventral striatum and in the right caudate nucleus in the PDD group ($P < 0.001$, corrected). Accordingly, we conclude that dementia in PD is associated with impaired mesolimbic and caudate dopaminergic function.

Keywords: 6-[^{18}F]fluoro-L-dopa; positron emission tomography; Parkinson's disease; Parkinson's disease with dementia

Abbreviations: AADC = aromatic aminoacid decarboxylase; DLB = dementia with Lewy bodies; Ki = ^{18}F-dopa influx constant; PD = Parkinson's disease without dementia; PDD = Parkinson's disease with dementia; ROI = region of interest; SN = substantia nigra; SPM = statistical parametric mapping; UPDRS = unified Parkinson's disease rating scale; VTA = ventral tegmental area

Introduction

The use of 6-[^{18}F]fluoro-L-dopa (^{18}F-dopa) with PET permits the study of presynaptic dopaminergic terminal function in the striatum *in vivo* in both healthy volunteers and Parkinson's disease (PD) patients. In PD, this technique has been used to provide a measure of disease severity and to identify individuals with early, and even preclinical, disease (Garnett *et al.*, 1987; Bhatt *et al.*, 1991; Brooks *et al.*, 1991; Burn *et al.*, 1992; Sawle *et al.*, 1992; Morrish *et al.*, 1995).

Although the main dopaminergic projections are nigrostriatal, extrastriatal dopamine terminals are also involved to varying extents in different phenotypes of idiopathic PD and other parkinsonian syndromes. Already, previous studies have reported the association between cognitive impairment and dopaminegic dysfunction in PD using ^{18}F-dopa PET and conventional region of interest (ROI) analysis (Holthoff-Detto *et al.*, 1997; Rinne *et al.*, 2000). However, accurate detection of dopaminergic changes in cortical and brainstem areas, where ^{18}F-dopa uptake constants are lower than those in the striatum, is unreliable using conventional ROI analysis, as an *a priori* judgement must be made about region size and

Table 1 *Clinical characteristics of patients and control groups*

Characteristics	Normal controls (n = 15)	Patients with Parkinson's disease	
		PD (n = 10)	PDD (n = 10)
Age (years)	67.4 ± 5.2	65.8 ± 6.7	66.1 ± 6.9
Sex (M/F)	4/11	2/8	7/3
Disease duration (years)	NA	6.6 ± 4.7	8.1 ± 6.0
Hoehn and Yahr rating score	NA	3.2 ± 0.6	3.2 ± 0.7
Motor UPDRS	NA	36.1 ± 16.1*	37.4 ± 12.8†
MMSE	29.2 ± 1.1	27.9 ± 2.2	20.4 ± 4.7‡

NA = not applicable; *n = 8; †n = 7; ‡$P < 0.001$ versus without dementia.

placement over potential sites of loss of dopaminergic function. As a consequence, the ROI approach is not suited for use as an exploratory technique with ^{18}F-dopa PET. Thus, we developed a technique for spatially normalizing ^{18}F-dopa influx (Ki) images, and have used statistical parametric mapping (SPM) to assess the extrastriatal uptake of ^{18}F-dopa in normal and PD brains (Ito *et al.*, 1999; Rakshi *et al.*, 1999; Nagano *et al.*, 2000).

In this study, we applied our normalization and SPM approach to equivalently disabled Parkinson's disease patients without (PD) and with (PDD) dementia in order to localize relative differences in their pathophysiologies on a voxel-by-voxel basis.

Material and methods

Subjects

Ten patients with idiopathic PD (six right dominant and four left dominant; mean age 65.8 ± 6.7 years) without dementia and 10 patients with PDD (seven right dominant and three left dominant; mean age 66.1 ± 6.9 years) were recruited from the Chubu National Hospital Neurology Clinic. All PD patients fulfilled UK Brain Bank criteria for diagnosis of this disorder. The PDD patients met the criteria for PDD, namely parkinsonism plus dementia, where the motor manifestations preceded the cognitive ones by at least 1 year (McKeith *et al.*, 1996). Although the PDD patients included some cases with a relatively high mini mental state examination (MMSE) score, all fulfilled Diagnostic and Statistical Manual (DSM) IV criteria for dementia. The 10 PD and 10 PDD patients were equivalently disabled, having a mean score of 3.2 ± 0.6 and 3.2 ± 0.7, respectively, on the Hoehn and Yahr rating scale. Motor unified Parkinson's disease rating scale (UPDRS) score was available for eight PD and seven PDD patients, and there was no significant difference between two groups. The PD and PDD patients without significant cerebral atrophy beyond what would be expected for age on MRI were selected for PET in order to minimize partial volume effects due to brain volume loss. Each patient was assessed clinically by neurologists before PET and at least 48 h after discontinuing their medications. The PDD patients in this study were given no specific treatment, such as acetylcholinesterase inhibitors, for their dementia. Details of the patients are shown in Table 1.

A separate group of 15 normal volunteers (mean age 67.4 ± 5.2 years) was recruited and scanned over the same time period. These 15 volunteers had no symptoms or signs suggestive of a neurological disorder and displayed no significant structural abnormalities except for normal age-related changes, such as dilated perivascular spaces, on their MRIs.

Permission to perform this study was obtained from the Ethical Committee of the Chubu National Hospital. All of the subjects gave written informed consents prior to PET scanning.

PET study

An oral bolus (100 mg) of carbidopa, a peripheral aromatic amino acid decarboxylase inhibitor, was given 1 h before scanning. Dynamic ^{18}F-dopa PET studies were performed using an ECAT EXACT HR47 (CTI/Siemens, Knoxville, Tenn., USA) in three-dimensional acquisition mode, which yielded 47 simultaneous planes, with an axial full-width half-maximum (FWMH) resolution of 4.8 mm and an in-plane resolution of 3.9 × 3.9 mm. An air cushion was inflated such that it moulded to the shape of the back of the head of each subject, thus minimizing head movements. Correction for tissue attenuation of 511 keV γ radiation was measured with a 10 min, two-dimensional transmission scan performed prior to the tracer injection using three retractable ^{68}Ga/^{68}Ge sources.

Eighty to 180 MBq of ^{18}F-dopa were infused intravenously into each subject over 30 s. Scanning began at the start of tracer injection. The protocol included 25 time frames (4 × 1 min, 3 × 2 min, 3 × 3 min, 15 × 5 min) over 94 min.

All of the subjects underwent high-resolution volumetric MRI with a Visart 1.5 T MRI (Toshiba, Tokyo, Japan). A field echo sequence protocol (TR: 20 ms; TE: 7 ms; flip angle: 35°) generated 1.5-mm thick sagittal images without slice gaps.

Functional mapping and spatial normalization of images

Data analysis was performed on a Sun workstation (Sun Microsystems, Silicon Valley, Calif., USA). In order to correct for head movement during scans, a dynamic file from each subject was divided into time frames and then each time frame was aligned to the mean image of all frames using the alignment program in SPM95.

The ^{18}F-dopa influx constant (Ki) image and integrated 'add image' were created using 'kronos' software developed by D. Bailey (MRC Cyclotron Unit, Hammersmith Hospital, London, UK) and implemented in IDL Image Analysis software (Research Systems, Inc., Boulder, Col., USA), based on the multiple time graphical analysis (MTGA) approach of Patlak and Blasberg (Patlak *et al.*, 1983, 1985). The 'add image' comprised integrated 30–94 min time frames of the ^{18}F-dopa dynamic images. We used the cerebellar tissue counts between 0 and 94 min post-injection as a reference tissue input function, and brain tissue activity on a voxel-by-voxel basis between 30 and 94 min to compute the gradient of the linear regression line representing Ki with the MTGA approach. The right and left cerebellar ROIs defining the input function were placed on each of three contiguous slices.

Using ANALYZE 7.0 software (Mayo Foundation, Baltimore, Md., USA), the scalp was edited from the MRI and the ^{18}F-dopa add image of each subject. The ^{18}F-dopa add image was then co-registered to each individual MRI using Automated Image Registration (AIR) software developed by Woods (Woods *et al.*, 1992, 1993). The Ki image was also co-registered to each individual MR image, using the same parameters as those used to co-register the respective ^{18}F-dopa add image to the MRIs.

The MRIs were transformed into standard stereotactic space of Talairach and Tournoux (Talairach *et al.*, 1988) using the normalization program in SPM95. We developed our normalization technique for ^{18}F-dopa images with SPM95 (Nagano *et al.*, 2000). Therefore, the MRI template provided in SPM95 was used for this normalization. The co-registered ^{18}F-dopa Ki images were then transformed into standard stereotactic space using the parameters of spatial normalization applied to the MRIs of each subject.

Statistical parametric mapping

Significant differences in mean regional Ki values between different groups were localized with SPM96 (Wellcome Department of Cognitive Neurology, London, UK) on a voxel-by-voxel basis. A Gaussian kernel of 8 × 8 × 8 mm (FWHM in the x, y and z planes, respectively) was applied to remove high-frequency noise from the images. Appropriate contrasts were used to derive the (unpaired) t statistic between the groups using the general linear model. The resulting set of voxel t values constitutes an SPM{t}, which is used to make inferences about regionally significant changes in Ki (Friston *et al.*, 1991). The SPM{t}s were transformed to maps of Z scores (SPM{Z}) for display purposes. The P values associated with regional differences in Ki were corrected for multiple dependent comparisons implicit in SPM96 using the theory of Gaussian fields. Maps of Z scores surviving a threshold of 2.33 ($P < 0.01$) and extent corrected $P < 0.05$ were generated to detect significant differences between patients and healthy controls. In contrast, for the comparison between the PD and PDD patients, maps of Z scores surviving a more conservative threshold of 3.09 ($P < 0.001$) and extent corrected $P < 0.05$ were applied.

ROI analysis

In order to calculate the mean value and standard deviation of Ki corresponding to each significant area on SPM{Z}, an ROI analysis was performed. As we previously reported, the automated ROI analysis was applicable to spatially normalized Ki images of ^{18}F-dopa across different cases, and its result was identical to conventional ROI analysis (Ito *et al.*, 1999; Nagano *et al.*, 2000). Therefore, ROIs were drawn on the MRI template in SPM95 and transferred to the spatially normalized Ki images. Considering the known dopaminergic projections in the human brain and the results of group comparison between PDD and normal controls with SPM, ROIs were defined for the caudate, putamen, ventral midbrain, amygdala, hippocampus and anterior cingulate cortex on each of three contiguous planes. The ROIs depicted on the templates were applied to each of the three adjacent planes of spatially normalized Ki images of each subject and mean regional Ki values were calculated for each individual. The mean regional Ki values between the groups were compared by analysis of variance (ANOVA) and *post hoc* Fisher's PLSD (protected least significant difference) to correct for multiple comparisons.

Results

SPM localized a significant reduction in mean ^{18}F-dopa Ki in the putamen bilaterally, right caudate nucleus and left ventral midbrain for the PD group compared with the normal controls ($P < 0.01$, corrected). The mean Ki of left caudate nucleus was also decreased, but the reduction failed to reach statistical significance ($P < 0.05$, corrected). Compared with the normal group, the PDD patients showed significant declines in ^{18}F-dopa uptake bilaterally in the caudate nucleus, putamen, midbrain and anterior cingulate area ($P < 0.01$, corrected). The corresponding SPMs and peak coordinates in SPM analysis are shown in Fig. 1 and Table 2. Compared with the PD group, the PDD patients showed consistent declines in ^{18}F-dopa Ki bilaterally in the anterior cingulate area 32 and ventral striatum and in the right caudate nucleus ($P < 0.001$, corrected). There were also similar trends bilaterally in the putamen and in the left caudate nucleus, but these did not reach statistical significance ($P < 0.05$, corrected). The declines in the ^{18}F-dopa Ki for the left amygdala also failed to reach statistical significance ($P < 0.01$, corrected). The

corresponding SPMs and peak coordinates in SPM analysis between PD and PDD are shown in Fig. 2 and Table 2. No significant increases in Ki were observed for either PD or PDD patients compared with the normal group.

The results of Ki measurements from the ROI analysis are shown in Fig. 3 and Table 3. Compared with the normal group, the PDD patients showed significant declines in ^{18}F-dopa Ki bilaterally in the caudate nucleus, putamen, ventral midbrain and anterior cingulate area. Compared with the PD group, the mean Ki values in the PDD group were further decreased in all regions and the reductions reached statistical significance in the caudate nucleus and putamen bilaterally, as well as in the left anterior cingulate area and left amygdala. There was also a similar trend in the right anterior cingulate area, although it was not statistically significant.

In order to clarify a statistical correlation between ^{18}F-dopa uptake and MMSE, significant correlations were localized with SPM96 on a voxel-by-voxel basis in 20 patients (both PD and PDD subjects). The MMSE score significantly correlated with the Ki values in the right caudate nucleus ($P < 0.001$, corrected). There were also similar trends bilaterally in the putamen, ventral striatum, anterior cingulate area and hippocampus, but these did not reach statistical significance ($P < 0.01$, corrected). The corresponding SPMs are shown in Fig. 4.

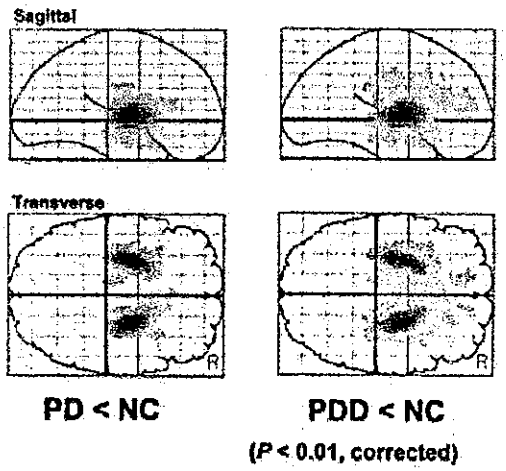

Fig. 1 SPMs showing the spatial distribution of significant regions ($P < 0.01$, corrected) where Ki decreased in PD (*left*) and PDD (*right*) compared with the normal control (NC). Images are shown as integrated projections along sagittal and transverse views of the Talairach and Tournoux brain atlas.

Discussion

Concomitant dementia represents a significant clinical problem in Parkinson's disease patients, its prevalence being estimated to be ~20% of all PD patients (Lieberman *et al.*, 1979; Brown *et al.*, 1984). Pathologically, dementia in Parkinson's disease has been attributed to direct involvement of the cortex by Lewy body (LB) pathology (Kosaka *et al.*, 1984, 1993), incidental Alzheimer's disease (Hakim *et al.*, 1979; Boller *et al.*, 1980), loss of cholinergic projections due to degeneration of the basal nucleus of Meynert (Whitehouse *et al.*, 1983; Gaspar *et al.*, 1984) and loss of mesolimbic and mesocortical dopaminergic projections due to degeneration of medial substantia nigra (SN) and ventral tegmental area (VTA) (Torack *et al.*, 1988; Rinne *et al.*, 1989). A previous clinicopathological study has reported that among 44 patients

Table 2 *Peak coordinates in SPM analysis*

P (corrected)	^{18}F-dopa Ki	Region	Coordinates (mm)			Z score
			x	*y*	*z*	
Comparison of PD with normal group						
0.000	1700	Rt caudate and putamen	24	–6	4	8.44
0.000	1536	Lt putamen	–26	–12	4	8.45
		Lt ventral midbrain	–12	–16	–12	3.38
Comparison of PDD with normal group						
0.000	7633	Rt caudate and putamen	24	–6	4	9.20
		Lt caudate and putamen	–26	–12	4	8.89
		Rt ventral midbrain	16	–18	–12	4.64
		Lt ventral midbrain	–10	–16	–12	3.59
		Rt ant cingulate	2	26	16	4.26
		Lt ant cingulate	–10	44	8	3.77
Comparison of PDD with PD						
0.000	181	Rt ventral striatum	16	4	–12	4.91
0.000	268	Rt caudate	16	4	8	4.36
0.000	210	Lt ventral striatum	–18	14	–12	4.62
		Rt ant cingulate	4	26	–8	3.99
		Lt ant cingulate	–8	44	12	5.02

Maximum peak coordinate for each anatomical region is listed. Rt, right; Lt, left; ant, anterior.

with PDD, 29% had Alzheimer's disease, 10% had numerous cortical LBs, 6% had a possible vascular cause and in 55% no definite pathologic cause was found. Owing to such heterogeneity in mechanisms of dementia in PD, the relationship of PDD to PD and to dementia with LBs (DLB) still requires clarification (Perry *et al.*, 1990; Mega *et al.*, 1996). Functional imaging with PET provides an objective means of revealing the pathophysiology of neurodegenerative diseases and supplements clinical diagnosis. Specifically, we have used PET to assess dopaminergic function, which is impaired in PDD and PD, in order to reveal their pathophysiology.

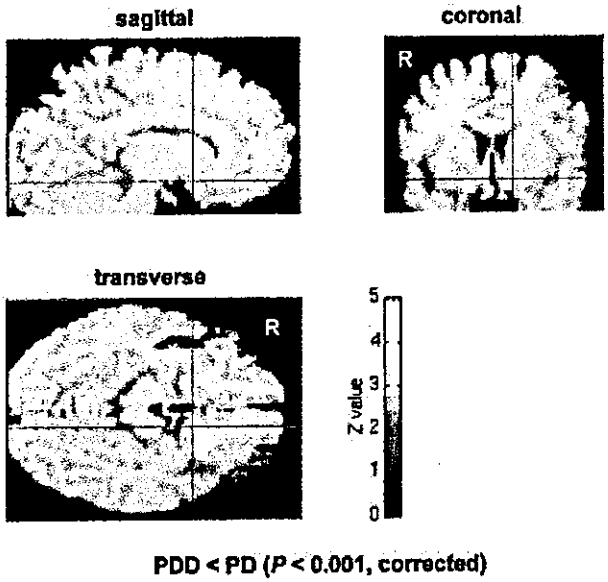

Fig. 2 Significant regions ($P < 0.001$, corrected) of decreased dopamine metabolism (Ki) in PDD compared with PD superimposed on a normalized brain MRI. SPM showed relative declines of ^{18}F-dopa uptake bilaterally in the anterior cingulate area and ventral striatum and in the right caudate nucleus.

With SPM, we found that the PDD group showed additional significant reductions in ^{18}F-dopa uptake in voxels distributed over the anterior cingulate area, ventral striatum bilaterally and the right caudate nucleus compared with non-demented PD patients. These findings are in line with *post mortem* studies that have demonstrated severe involvement of the mesolimbic and mesocortical dopaminergic system in addition to the nigrostriatal system in PDD patients (Rinne *et al.*, 1989). Mesolimbic dopamine projections, including those to the anterior cingulate area and ventral striatum, originate from cell bodies in the medial SN and midbrain VTA. Therefore, this study reinforces our view that dementia in PD is associated with involvement of the medial part of the SN and VTA.

The MMSE score in the combined group of PD and PDD patients significantly correlated with the Ki values in the right caudate nucleus; there were also similar trends bilaterally in the putamen, ventral striatum, anterior cingulate area and hippocampus. Correspondingly, the association between the degree of cognitive impairment and ^{18}F-dopa uptake in the caudate nucleus and medial frontal cortex has been reported in PD patients via PET (Holthoff-Detto *et al.*, 1997; Rinne *et al.*, 2000). In addition, the correlation between the orbitofrontal binding site density of dopamine transporter and mentation scores of the UPDRS in early PD has been reported (Ouchi *et al.*, 1999), as has the correlation between the right caudate binding site density of dopamine transporter and frontal executive performance (Marie *et al.*, 1999). These findings suggest that caudate, mesolimbic and mesocortical dopaminergic dysfunction plays an important role in the cognitive impairment of PD. There may also be an additional association with temporo-parietal dysfunction, as FDG PET

Table 3 *Mean regional Ki values in normal, PD and PDD*

	Ki/min											
	Rt caudate	Lt caudate	Rt putamen	Lt putamen	Rt ventral midbrain	Lt ventral midbrain	Rt ant cingulate	Lt ant cingulate	Rt amygdala	Lt amygdala	Rt hippo-campus	Lt hippo-campus
Normal (n =15)												
Mean	0.0092	0.0086	0.0093	0.0092	0.0027	0.0029	0.0016	0.0016	0.0037	0.0034	0.0023	0.0024
SD	0.0011	0.0011	0.0010	0.0012	0.0008	0.0010	0.0004	0.0006	0.0004	0.0009	0.0004	0.0004
PD (n = 10)												
Mean	0.0069	0.0070	0.0042	0.0042	0.0022	0.0021	0.0015	0.0016	0.0035	0.0038	0.0025	0.0024
SD	0.0012	0.0014	0.0009	0.0008	0.0007	0.0005	0.0006	0.0005	0.0005	0.0009	0.0005	0.0005
P values*	0.002	0.008	<0.001	<0.001	n.s.	0.023	n.s.	n.s.	n.s.	n.s.	n.s.	n.s.
PDD (n = 10)												
Mean	0.0051	0.0056	0.0031	0.0032	0.0017	0.0017	0.0011	0.0011	0.0032	0.0027	0.0020	0.0023
SD	0.0016	0.0016	0.0011	0.0008	0.0005	0.0004	0.0003	0.0003	0.0009	0.0008	0.0006	0.0008
P values*	<0.001	<0.001	<0.001	<0.001	0.003	0.001	0.031	0.021	n.s.	n.s.	n.s.	n.s.
P values†	0.008	0.021	0.029	0.045	n.s.	n.s.	n.s.	0.044	n.s.	0.019	n.s.	n.s.

*Comparison of PD or PDD with normal group; †comparison of PDD with PD. Lt, left; Rt, right; n.s., not significant.

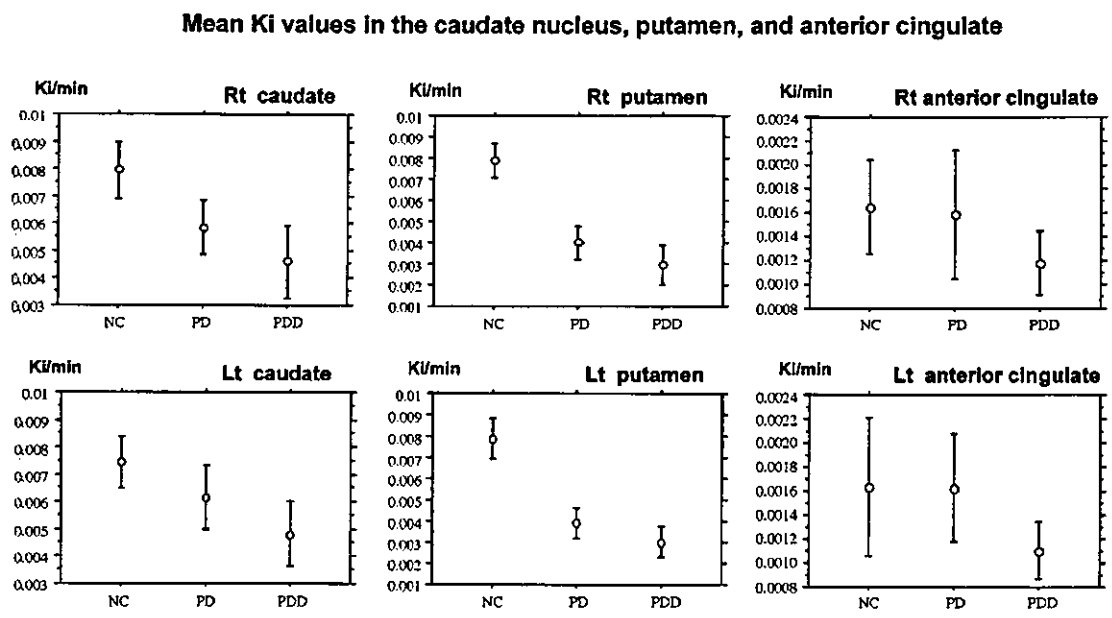

Fig. 3 The mean Ki values in the caudate nucleus, putamen and anterior cingulate area for the normal control (NC), PD and PDD patients in the ROI analysis. Bars are standard deviations. The mean Ki value in the anterior cingulate area decreased only for PDD compared with normal control. In contrast to this, the mean Ki values in the caudate nucleus and putamen decreased for both PD and PDD.

has shown glucose hypometabolism in these areas in PDD (Schapiro *et al.*, 1993; Vander *et al.*, 1997).

The anterior cingulate is within the areas that show the most obvious pathological changes in DLB and PDD (Pellise *et al.*, 1996). Furthermore, atrophy of the cingulate cortex has been noted pathologically in PD (Braak *et al.*, 1995). For this reason, our cases of PD and PDD were carefully selected to have non-atrophic MRIs, in order to minimize any partial volume effects. Although the potential cortical pathology could be a potential explanation for reduced ^{18}F-dopa uptake in the anterior cingulate, our results suggest that demented PD patients have reduced cingulate aromatic amino-acid decarboxylase (AADC) activity before focal cerebral atrophy can be detected.

There were a few differences in statistical significance between SPM and the automated ROI analysis. We believe that these differences probably arose as a result of the different statistical approaches used in the two analyses. SPM is performed on a voxel basis and uses the general linear model and the theory of continuous random fields to correct for multiple comparisons, while Kis from ROIs were interrogated with ANOVA and *post hoc* Fisher's PLSD.

Previously, we reported an increased Ki in early PD and an unchanged Ki in advanced PD in the cingulate cortex compared with normal controls (Rakshi *et al.*, 1999). In this study, the Ki in the cingulate cortex did not show any significant change in the PD group compared with the normal group. These results are considered to be compatible with our previous report, because the PD group in this study consisted of established PD cases with a mean score of 3.2 ± 0.6 on the Hoehn and Yahr rating scale.

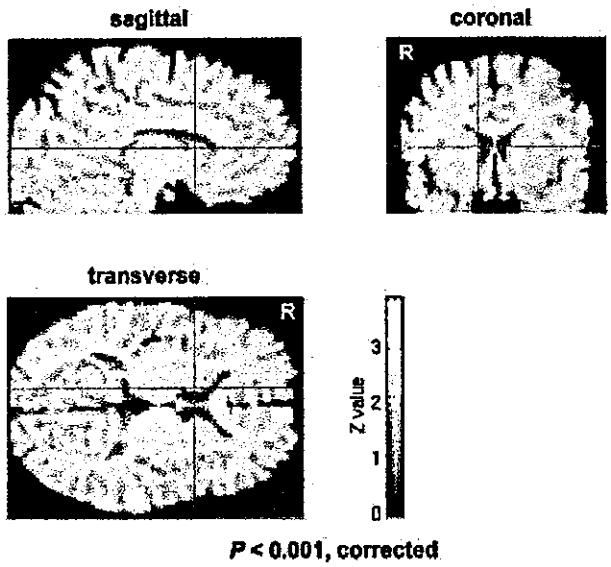

Fig. 4 Significant regions ($P < 0.001$, corrected) of correlation between ^{18}F-dopa uptake and MMSE in the combined group of PD and PDD patients, superimposed on a normalized brain MRI. The MMSE score positively correlated with the Ki values in the right caudate nucleus.

^{18}F-dopa is decarboxylated by AADC to yield ^{18}F-dopamine (Tison *et al.*, 1991). Therefore, the Ki value is considered to be an index of AADC activity. The normal subjects had relatively high Ki values within the midbrain, amygdala, hippocampus and cingulate cortex, as well as in

the caudate nucleus and putamen. These regions all correspond to dopaminergic projection areas in the brain; however, recent studies have suggested that noradrenergic and serotoninergic neurones also display AADC activity (Arai *et al.*, 1996). Accordingly, the findings in our study could also reflect possible impairments of the noradrenergic and serotoninergic projections. Despite this possibility, we believe that the non-selectivity of ^{18}F-dopa is not a disadvantage, but allows sensitive detection of monoaminergic dysfunction.

So far, the function of pre- and postsynaptic cholinergic termini has been evaluated in Parkinson's disease using [^{123}I]iodobenzovesamicol (IBVM) single photon emission computed tomography (SPECT) (Kuhl *et al.*, 1996) and ^{11}C-*N*-methyl-4-piperidyl benzilate (NMPB) PET (Asahina *et al.*, 1998), respectively. These studies have suggested that cholinergic dysfunction might contribute to the cognitive impairment observed in Parkinson's disease. Therefore, to clarify the relation between dopaminergic and cholinergic dysfunction in Parkinson's disease, further comparative investigation is required.

This study demonstrates the impairment of striatal and extrastriatal function *in vivo* in PDD. The application of SPM to ^{18}F-dopa PET enables objective localization of impairments in monoaminergic function throughout the brain at a voxel level, and allows for comparisons of the regional differences in monoaminergic metabolism between PD and related disorders, including DLB. We believe that loss of mesolimbic and mesocortical dopaminergic projections is also likely to play an important role in the pathophysiology of DLB, which is included within the spectrum of Lewy body disease as well as PD and PDD.

Conclusion

In this study we have demonstrated a significant dysfunction in both the striatal and extrastriatal regions in PD patients with super-added dementia. These findings are consistent with the hypothesis that impairment of mesolimbic and caudate dopaminergic function plays an important role in the dementia of PD.

Acknowledgements

This study was supported by the fund for Comprehensive Research of Aging and Health and the fund for Brain Science from the Ministry of Welfare, Japan.

References

Arai R, Karasawa N, Nagatsu I. Aromatic L-amino acid decarboxylase is present in serotonergic fibers of the striatum of the rat. A double-labeling immunofluorescence study. Brain Res 1996; 706: 177–9.

Asahina M, Suhara T, Shinotoh H, Inoue O, Suzuki K, Hattori T. Brain muscarinic receptors in progressive supranuclear palsy and Parkinson's disease: a positron emission tomographic study. J Neurol Neurosurg Psychiatry1998; 65: 155–63.

Bhatt MH, Snow BJ, Martin WR, Pate BD, Ruth TJ, Calne DB. Positron emission tomography suggests that the rate of progression of idiopathic parkinsonism is slow. Ann Neurol 1991; 29: 673–7.

Boller F, Mizutani T, Roessmann U, Gambetti P. Parkinson disease, dementia, and Alzheimer disease: clinicopathological correlations. Ann Neurol 1980; 7: 329–35.

Braak H, Braak E, Yilmazer D, Schultz C, de Vos RA, Jansen EN. Nigral and extranigral pathology in Parkinson's disease. [Review]. J Neural Transm Suppl 1995; 46: 15–31.

Brooks DJ. Detection of preclinical Parkinson's disease with PET. Neurology 1991; 41 (5 Suppl 2): 24–7.

Brown RG, Marsden CD. How common is dementia in Parkinson's disease? Lancet 1984; 2: 1262–5.

Burn DJ, Mark MH, Playford ED, Maraganore DM, Zimmerman TR, Duvoisin RC, et al. Parkinson's disease in twins studied with ^{18}F-dopa and positron emission tomography. Neurology 1992; 42: 1894–900.

Friston KJ, Frith CD, Liddle PF, Frackowiak RS. Comparing functional (PET) images: the assessment of significant change. J Cereb Blood Flow Metab 1991; 11: 690–9.

Garnett ES, Lang AE, Chirakal R, Firnau G, Nahmias C. A rostrocaudal gradient for aromatic acid decarboxylase in the human striatum. Can J Neurol Sci 1987; 14 (3 Suppl): 444–7.

Gaspar P, Gray F. Dementia in idiopathic Parkinson's disease. A neuropathological study of 32 cases. Acta Neuropathol (Berl) 1984; 64: 43–52.

Hakim AM, Mathieson G. Dementia in Parkinson disease: a neuropathologic study. Neurology 1979; 29: 1209–14.

Holthoff-Detto VA, Kessler J, Herholz K, Bonner H, Pietrzyk U, Wurker M, et al. Functional effects of striatal dysfunction in Parkinson disease. Arch Neurol 1997; 54: 145–50.

Ito K, Morrish PK, Rakshi JS, Uema T, Ashburner J, Bailey DL, et al. Statistical parametric mapping with 18F-dopa PET shows bilaterally reduced striatal and nigral dopaminergic function in early Parkinson's disease. J Neurol Neurosurg Psychiatry 1999; 66: 754–8.

Kosaka K. Dementia and neuropathology in Lewy body disease. Adv Neurol 1993; 60: 456–63.

Kosaka K, Yoshimura M, Ikeda K, Budka H. Diffuse type of Lewy body disease: progressive dementia with abundant cortical Lewy bodies and senile changes of varying degree—a new disease? Clin Neuropathol 1984; 3: 185–92.

Kuhl DE, Minoshima S, Fessler JA, Frey KA, Foster NL, Ficaro EP, et al. In vivo mapping of cholinergic terminals in normal aging, Alzheimer's disease, and Parkinson's disease. Ann Neurol 1996; 40: 399–410.

Lieberman A, Dziatolowski M, Kupersmith M, Serby M, Goodgold A, Korein J, et al. Dementia in Parkinson disease. Ann Neurol 1979; 6: 355–9.

Marie RM, Barre L, Dupuy B, Viader F, Defer G, Baron JC.

Relationships between striatal dopamine denervation and frontal executive tests in Parkinson's disease. Neurosci Lett 1999; 260: 77–80.

McKeith IG, Galasko D, Kosaka K, Perry EK, Dickson DW, Hansen LA, et al. Consensus guidelines for the clinical and pathologic diagnosis of dementia with Lewy bodies (DLB): report of the consortium on DLB international workshop. [Review]. Neurology 1996; 47: 1113–24.

Mega MS, Masterman DL, Benson DF, Vinters HV, Tomiyasu U, Craig AH, et al. Dementia with Lewy bodies: reliability and validity of clinical and pathologic criteria. Neurology 1996; 47: 1403–9.

Morrish PK, Sawle GV, Brooks DJ. Clinical and [^{18}F] dopa PET findings in early Parkinson's disease. J Neurol Neurosurg Psychiatry 1995; 59: 597–600.

Nagano AS, Ito K, Kato T, Arahata Y, Kachi T, Hatano K, et al. Extrastriatal mean regional uptake of fluorine-18-FDOPA in the normal aged brain – an approach using MRI-aided spatial normalization. Neuroimage 2000; 11: 760–6.

Ouchi Y, Yoshikawa E, Okada H, Futatsubashi M, Sekine Y, Iyo M, et al. Alterations in binding site density of dopamine transporter in the striatum, orbitofrontal cortex, and amygdala in early Parkinson's disease: compartment analysis for beta-CFT binding with positron emission tomography. Ann Neurol 1999; 45: 601–10.

Patlak CS, Blasberg RG. Graphical evaluation of blood-to-brain transfer constants from multiple-time uptake data. Generalizations. J Cereb Blood Flow Metab 1985; 5: 584–90.

Patlak CS, Blasberg RG, Fenstermacher JD. Graphical evaluation of blood-to-brain transfer constants from multiple-time uptake data. J Cereb Blood Flow Metab 1983; 3: 1–7.

Pellise A, Roig C, Barraquer-Bordas LI, Ferrer I. Abnormal, ubiquitinated cortical neurites in patients with diffuse Lewy body disease. Neurosci Lett 1996; 206: 85–8.

Perry PH, Irving D, Blessed G, Fairbairn A, Perry EK. Senile dementia of Lewy body type. J Neurol Sci 1990; 95: 119–39.

Rakshi JS, Uema T, Ito K, Bailey DL, Morrish PK, Ashburner J, et al. Frontal, midbrain and striatal dopaminergic function in early and advanced Parkinson's disease. A 3D [^{18}F]dopa-PET study. Brain 1999; 122: 1637–50.

Rinne JO, Rummukainen J, Paljarvi L, Rinne UK. Dementia in Parkinson's disease is related to neuronal loss in the medial substantia nigra. Ann Neurol 1989; 26: 47–50.

Rinne JO, Portin R, Ruottinen H, Nurmi E, Bergman J, Haaparanta M, et al. Cognitive impairment and the brain dopaminergic system in Parkinson disease: [^{18}F]fluorodopa positron emission tomographic study. Arch Neurol 2000; 57: 470–5.

Sawle GV, Wroe SJ, Lees AJ, Brooks DJ, Frackowiak RS. The identification of presymptomatic parkinsonism; clinical and ^{18}F-dopa positron emission tomography studies in an Irish kindred. Ann Neurol 1992; 32: 609–17.

Schapiro MB, Pietrini P, Grady CL, Ball MJ, DeCarli C, Kumar A, et al. Reductions in parietal and temporal cerebral metabolic rates for glucose are not specific for Alzheimer's disease. J Neurol Neurosurg Psychiatry 1993; 56: 859–64.

Talairach J, Tournoux P. Co-planar stereotaxic atlas of the human brain. Stuttgart: Thieme; 1988.

Tison F, Normand E, Jaber M, Aubert I, Bloch B. Aromatic L-amino-acid decarboxylase (DOPA decarboxylase) gene expression in dopaminergic and serotoninergic cells of the rat brainstem. Neurosci Lett 1991; 127: 203–6.

Torack RM, Morris JC. The association of ventral tegmental area histopathology with adult dementia. Arch Neurol 1988; 45: 497–501.

VanderBorght T, Minoshima S, Giordani B, Foster NL, Frey KA, Berent S, et al. Cerebral metabolic differences in Parkinson's and Alzheimer's diseases matched for dementia severity. J Nucl Med 1997; 38: 797–802.

Whitehouse PJ, Hedreen JC, White CL 3rd, Price DL. Basal forebrain neurons in the dementia of Parkinson disease. Ann Neurol 1983; 13: 243–8.

Woods RP, Cherry SR, Mazziotta JC. Rapid automated algorithm for aligning and reslicing PET images. J Comput Assist Tomogr 1992; 16: 620–33.

Woods RP, Mazziotta JC, Cherry SR. MRI-PET registration with automated algorithm. J Comput Assist Tomogr 1993; 17: 536–46.

Received May 14, 2001. Revised November 23, 2001.
Second revision January 17, 2002. Accepted January 24, 2002

DOI 10.1007/s00702-002-0753-0
J Neural Transm (2002) 109: 1433–1443

Journal of Neural Transmission
Printed in Austria

A comparison of the progression of early Parkinson's disease in patients started on ropinirole or L-dopa: an ^{18}F-dopa PET study

J. S. Rakshi[1], N. Pavese[1], T. Uema[1], K. Ito[1], P. K. Morrish[1], D. L. Bailey[1], and D. J. Brooks[1,2]

[1]MRC Clinical Sciences Centre Imperial College School of Medicine, Hammersmith Hospital, London, and
[2]The Institute of Neurology, Queen Square, London, United Kingdom

Received March 11, 2002; accepted April 2, 2002
Published online July 26, 2002;

Summary. *Objective:* To study the relative rates of progression of early Parkinson's disease (PD) in patients started on a dopamine agonist, ropinirole, or L-dopa. *Methods:* A double-blind study of 45 early PD patients [mean age 61 ± 9.8 SD and mean symptom duration, 26 ± 16 SD months] randomized 2:1 (ropinirole:L-dopa). Supplementary L-dopa was allowed if, during the trial, there was lack of a therapeutic effect. ^{18}F-dopa PET scans were performed at baseline (n = 45) and 2 years (n = 37). *Results:* At two years, the mean percentage reduction in putamen ^{18}F-dopa uptake (Ki^o) was not significantly different between the two groups (13% ropinirole, n = 28 versus 18% L-dopa, n = 9). *Conclusions:* We found no significant overall difference in underlying PD progression, after two years treatment, between patients groups. In summary, ^{18}F-dopa PET can be employed to objectively evaluate the effect of potential neuroprotective agents on dopaminergic function.

Keywords: ^{18}F-dopa PET, Parkinson's disease progression, ropinirole, neuroprotection, L-dopa toxicity.

Introduction

Parkinson's disease (PD) is a progressive neurodegenerative movement disorder characterised by bradykinesia, rigidity and tremor. The pathology targets dopaminergic neurones in the pars compacta of the substantia nigra leading to cell loss and Lewy body inclusions (Gibb, 1988). This in turn results in reduced striatal dopamine levels, putamen being more affected than caudate (Kish, 1988).

Although L-dopa is an effective symptomatic treatment of PD, in vitro studies have raised the possibility that it might be neurotoxic to remaining

dopaminergic neurones (Alexander, 1997; Graham, 1978; Mena, 1992, 1993; Michel, 1990; Newcomer, 1995). Consequently, attention has turned to potential neuroprotective or disease-modifying agents that could slow or halt PD progression. Dopamine agonists exert their antiparkinsonian effect by directly stimulating dopamine receptors. Their early use as a substitute for L-dopa avoids the production of hydrogen peroxide and hydroxyl free radicals resulting from oxidation of exogenous dopamine to DOPAC by monoamine oxidase B. In addition, they act on pre-synaptic dopamine D_2 autoreceptors producing down-regulation of endogenous dopamine synthesis, release and turnover. One could speculate, therefore, that dopamine agonists might exert a disease-modifying effect in PD by reducing oxidative stress. Indeed, pre-clinical studies have raised the possibility that dopamine agonists might afford protection to dopaminergic neurones by reducing basal ganglia glutamate levels and by acting as free-radical scavengers and anti-oxidants (Asanuma, 1995; Felten, 1992; Gassen, 1996; Iiada, 1999; Ogawa, 1994).

An attempt has already been made to assess the possible neuro-protective or disease modifying effect of a therapeutic agent in PD. The DATATOP study (Parkinson Study Group, 1989, 1993), however, highlighted the problems of using clinical assessment as a measure of disease progression because of the confounding effects of symptomatic benefit (Schulzer, 1992). To avoid this confound, one could assess patients following a washout period of their medication at the end of the study. The optimum duration of the washout period, however, is unclear, and would require patients being off medication for 2 or more weeks. An alternative method of objectively assessing PD progression would therefore be more desirable.

^{18}F-dopa PET enables the functional integrity of striatal and extra-striatal dopaminergic nerve terminals to be assessed in vivo in PD (Brooks, 1990; Garnett, 1983; Martin, 1989; Rakshi, 1999). Previous PET studies have demonstrated reduced putamen ^{18}F-dopa uptake with relative preservation of caudate dopaminergic function in PD (Brooks, 1990; Garnett, 1983). Furthermore, it has been shown that, with ^{18}F-dopa PET, it is possible to demonstrate progressive loss of dopamine terminal function in Parkinson's disease patients over a 2-year period (Morrish, 1996, 1998). Our study was designed to take this a step further by studying the relative rates of progression of early PD over 2 years in a group of patients randomised 2:1 to either dopamine agonist, ropinirole or L-dopa monotherapy. The 2:1 randomisation was chosen because these patients were studied in parallel with a larger multinational clinical study, which had the same randomisation (Rascol, 2000).

Ropinirole is a novel, non-ergoline dopamine agonist that is highly specific for dopamine D_2-like receptors, and has little affinity for D_1 or serotonin receptors (Eden, 1991). It acts at post-synaptic dopamine D_2-like receptors, leading to symptomatic efficacy, and also at pre-synaptic dopamine D_2 autoreceptors suppressing endogenous dopamine levels (Fears, 1994). It is licensed for use in all stages of PD. A recent multinational study (Rascol, 2000), has shown ropinirole to be an effective symptomatic treatment in early PD for up to five years and its early use results in a significantly lower prevalence of dyskinesias compared to L-dopa.

Material and methods

Patients

45 patients with early PD [mean age 61 ± 9.8 SD and mean symptom duration, 26 ± 16 SD months] were recruited from 11 regional centres in the UK and France. All patients except one fulfilled the UK Parkinson's disease Brain Bank criteria for the clinical diagnosis of idiopathic Parkinson's disease. One recruited patient, however, on clinical assessment (atypical tremor with no rigidity or bradykinesia) and prior to both his baseline, and 2 year PET scans, did not fulfil the UK Brain Bank criteria. Patients previously treated with low-to-moderate doses of L-dopa or a dopamine agonist for up to three months were eligible provided that they discontinued such treatment for at least 2 weeks prior to screening. Concomitant selegiline (L-deprenyl) was not allowed. After a 1-week screening period during which patients received placebo, patients were randomized in a 2:1 ratio to ropinirole or L-dopa monotherapy. The dosage of medication for each patient was then titrated according to clinical response. The maximum daily doses permitted were 24 mg of ropinirole or 1,200 mg of L-dopa. If there was a lack of therapeutic effect despite the highest tolerated dose level, recruiting investigators could add supplementary L-dopa in an open-label fashion while the patient remained on double-blind study medication.

Patients travelled to the Hammersmith Hospital for their serial ^{18}F-dopa PET scans at baseline (within 6 months of entry into study) and 2 years. Each patient was clinically assessed with the motor UPDRS and H & Y rating scales (Fahn, 1987; Hoehn, 1967), by one of three observers JSR, NP, or PKM at least 12 h after stopping their medication (practically defined "off" motor score) on the morning of their PET scan. On clinical assessment of the 44 PD patients, prior to baseline scan, the mean Hoehn and Yahr (H&Y) score was 1.8 ± 0.5 and the mean score on the motor subscale of the Unified Parkinson's Disease Rating Scale (UPDRS) was 13 ± 6.5. All patients gave written informed consent after a full explanation of the procedure. Permission to perform these studies was granted by the Ethics Committee of the Hammersmith Hospital Trust, London, UK and the Administration of Radioactive Substances Advisory Committee (ARSAC), UK.

Scanning protocol

Each subject had their medication stopped 12 hours before and were fasted on the morning of their ^{18}F-dopa PET. In addition, all subjects received an oral bolus of 150 mg of carbidopa, a peripheral dopa decarboxylase (DDC) inhibitor, and 400 mg of entacapone, a peripheral catechol-O-methyl transferase (COMT) inhibitor (Orion Farmos Pharmaceuticals Espoo, Finland) 1 hour before their PET scan. The administration of a COMT inhibitor reduces the non-specific background activity by inhibiting peripheral ^{18}F-dopa metabolism to 3-O-methyl-^{18}F-dopa. In practical terms, this increases the contrast between striatal and cortical reference tissue making it easier to place regions of interest (ROI's) over the striatum. Furthermore, it increases ^{18}F-dopa influx rate constants estimated with a reference tissue input function (Ishikawa, 1996; Sawle, 1994).

Patients had either serial 2D ^{18}F-dopa PET scans on the ECAT 931 scanner or serial 3D ^{18}F-dopa PET scans on the ECAT 953B scanner (CTI/Siemens, Knoxville, TN, USA) using protocols and reconstruction methods previously described (Bailey, 1992, 1994; Morrish, 1998; Rakshi, 1996). From October 1994, the more sensitive 3D-mode scanning was used for new patients; patients previously scanned with a 2D-mode scanner continued to be scanned in the same way. Consequently, 17 patients had two 2D and 20 patients had two 3D ^{18}F-dopa PET scans. All patients received between 110–200 MBq of ^{18}F-dopa in 10 ml of normal saline solution as an intravenous bolus infused over 30 seconds. The subjects were positioned such that the orbitomeatal line was parallel to the transaxial plane of the tomograph and head position was carefully monitored with a video camera and by direct observation throughout the scan.

Data analysis

We employed a region-of-interest (ROI) approach to sample putamen activity. ^{18}F-dopa uptake was expressed as an influx rate constant (Ki^o) and was calculated from putamen tissue counts 25–94 min post-injection using multiple time graphical analysis (Patlak, 1985) with occipital tissue counts as the input function (Brooks, 1990). We applied a standard ROI template: each dorsal putamen was sampled with an elliptical region 10 × 24 mm aligned to its long axis, with reference to the stereotaxic atlas of Talairach and Tournoux (1988). Putamen ROIs were placed over three contiguous transaxial planes for 3D-mode datasets and over two contiguous planes for 2D-mode datasets giving a comparable total axial plane thickness (~18 mm) for the two cameras (Rakshi, 1999). To generate the input function, we sampled right and left occipital lobes with two circular regions of 32-mm diameter placed on the same three (3D mode) or two (2D mode) contiguous transaxial planes as those selected for dorsal putament. All ROIs were placed manually using in-house software written in IDL image analysis software (Research Systems, Inc., Boulder, CO, USA). Image analysis was performed by JSR who was blinded to treatment assignment. ROI's were independently defined for the follow-up scans for each subject. For each patient, we calculated the putamen Ki^o (averaged right and left putamen Ki^o values) at baseline and 2 years. We also calculated best putamen Ki^o values (highest individual putamen Ki^o value out of right and left putamen from each subject's baseline scan) and worst putament Ki^o values (lowest individual putamen Ki^o value out of right and left putamen from each subject's baseline scan). We then calculated percentage change in putamen Ki^o, best putamen Ki^o and worst putamen Ki^o between corresponding baseline and 2-year scan. The mean percentage change in putamen Ki^o for the ropinirole and L-dopa patient groups was then calculated. Analysis of variance using SAS software was used to compare the results from the two treatment groups at 2 years.

Results

Patients

The number of patients at each study time point, in each group, is illustrated in the flow chart (Fig. 1). 45 patients underwent a baseline ^{18}F-dopa PET scan within 6 months of trial recruitment. Six patients withdrew from the study before their second scan (two patients developed unrelated medical problems and were withdrawn by their recruiting centre and four patients withdrew consent for a second PET scan). Therefore, 39 out of the original 45 patients had two serial PET scans. Data from two of the 39 patients, however, had to be excluded from the final analysis. One of these patient's had a non-evaluable scan because of incomplete PET data acquisition and the second patient, had two ^{18}F-dopa PET scans yielding normal putamen Ki^o values over the 2-year period (this was the patient who did not fulfil the UK Brain Bank criteria for clinical PD).

At 2 years, of the 37 patients with evaluable serial scans, 28 had been randomized to ropinirole and nine to L-dopa monotherapy (Fig. 1). By chance, a proportionately greater number of the subjects who withdrew and the one subject with a non-evaluable scan had been randomised to L-dopa.

There was no significant difference in mean putamen Ki^o values between treatment groups at baseline (0.0069 ± 0.0015 min^{-1} – ropinirole: 0.0074 ± 0.0019 min^{-1} – L-dopa).

A total of 19 of the 37 patients (51%) assessed at the 2-year follow-up remained on monotherapy. (i.e. were not taking supplementary L-dopa).